Facies analysis, stratigraphy and marine vertebrate assemblage of the lower Miocene Chilcatay Formation at Ullujaya (Pisco basin, Peru)

C. Di Celma, E. Malinverno, A. Collareta, G. Bosio, K. Gariboldi, O. Lambert, W. Landini, P.P. Pierantoni, A. Gioncada, I.M. Villa, G. Coletti, C. de Muizon, M. Urbina & G. Bianucci

Science

Facies analysis, stratigraphy and marine vertebrate assemblage of the lower Miocene Chilcatay Formation at Ullujaya (Pisco basin, Peru)

C. Di Celma[a], E. Malinverno[b], A. Collareta[c], G. Bosio[b], K. Gariboldi[c], O. Lambert[d], W. Landini[c], P.P. Pierantoni[a], A. Gioncada[c], I.M. Villa[b], G. Coletti[b], C. de Muizon[e], M. Urbina[f] and G. Bianucci[c]

[a]Scuola di Scienze e Tecnologie, Università di Camerino, Camerino, Italy; [b]Dipartimento di Scienze dell'Ambiente e della Terra, Università di Milano-Bicocca, Milano, Italy; [c]Dipartimento di Scienze della Terra, Università di Pisa, Pisa, Italy; [d]D.O. Terre et Histoire de la Vie, Institut Royal des Sciences Naturelles de Belgique, Brussels, Belgium; [e]Département Origines et Évolution, Muséum national d'Histoire naturelle, Centre de Recherche sur la Paléobiodiversité et les Paléoenvironnements – CR2P (CNRS, MNHN, UPMC, Sorbonne Université), Paris, France; [f]Departamento de Paleontologia de Vertebrados, Museo de Historia Natural-UNMSM, Lima, Peru

ABSTRACT

This paper is the first integrated account of the sedimentology, stratigraphy, and vertebrate paleontology for the marine strata of the Chilcatay Formation exposed at Ullujaya, Pisco basin (southern Peru). An allostratigraphic framework for the investigated strata was established using geological mapping (1:4000 scale) and conventional sedimentary facies analysis and resulted in recognition of two unconformity-bounded allomembers (designated Ct1 and Ct2 in ascending order). The chronostratigraphic framework is well constrained by integration of micropaleontological data and isotope geochronology and indicates deposition during the early Miocene. The marine vertebrate fossil assemblage is largely dominated by cetaceans (odontocetes), whereas isolated teeth and spines indicate a well-diversified elasmobranch assemblage. Our field surveys, conducted to evaluate the paleontological sensitivity of the investigated strata, indicate that vertebrate remains only came from a rather restricted stratigraphic interval of the Ct1 allomember and reveal the high potential for these sediments to yield abundant and scientifically significant fossil assemblages.

1. Introduction

The Chilcatay Formation, southern Peru, has received wide attention in the past few years due to numerous significant discoveries of fossil cetaceans (Bianucci, Urbina, & Lambert, 2015; Lambert et al., 2017; Lambert, Bianucci, & Urbina, 2014; Lambert, de Muizon, & Bianucci, 2015). By contrast, published sedimentological and stratigraphical interpretations on this unit are sparse and mostly limited to preliminary studies based on selected outcrops (DeVries & Schrader, 1997; León, Aleman, Torres, Rosell, & De La Cruz, 2008; Wright, Dunbar, Allen, & Baker, 1988). As a result, most studies of fossil vertebrates from the Chilcatay Formation have suffered from a lack of a detailed stratigraphic information and the accurate placement of these discoveries into a proper stratigraphic context remains a largely unresolved issue bearing upon uncertain intraformational correlations and poor age control.

This paper is part of a broader effort to complete detailed mapping and to provide more accurate stratigraphic and age constraints for fossil-bearing localities of the Pisco Basin (Brand, Urbina, Chadwick, DeVries, & Esperante, 2011; Di Celma et al., 2016a, 2016b, 2017; Gariboldi et al., 2017). In this study, stratigraphic architecture of a proximal portion of the Chilcatay Formation and fossil distribution within its strata have been constrained by the integration of geological field mapping, section measuring, facies analysis, and age estimates from both isotope geochronology and microfossil biostratigraphy. The data reported here provide a crucial background for future comparisons among Chilcatay localities and a first picture of the spatial and stratigraphic distribution of the fossil marine vertebrates and of the quantitative and qualitative composition of the whole vertebrate assemblage.

2. Geological and stratigraphic setting

According to Thornburg and Kulm (1981), two trench-parallel structural ridges were formed on the continental shelf and upper slope of the Peruvian margin during Late Cretaceous-early Palaeogene time, namely the Outer Shelf High and the Upper Slope Ridge. These two ridges subdivided the Peruvian offshore into a series of sedimentary basins (Figure 1(a)), which may
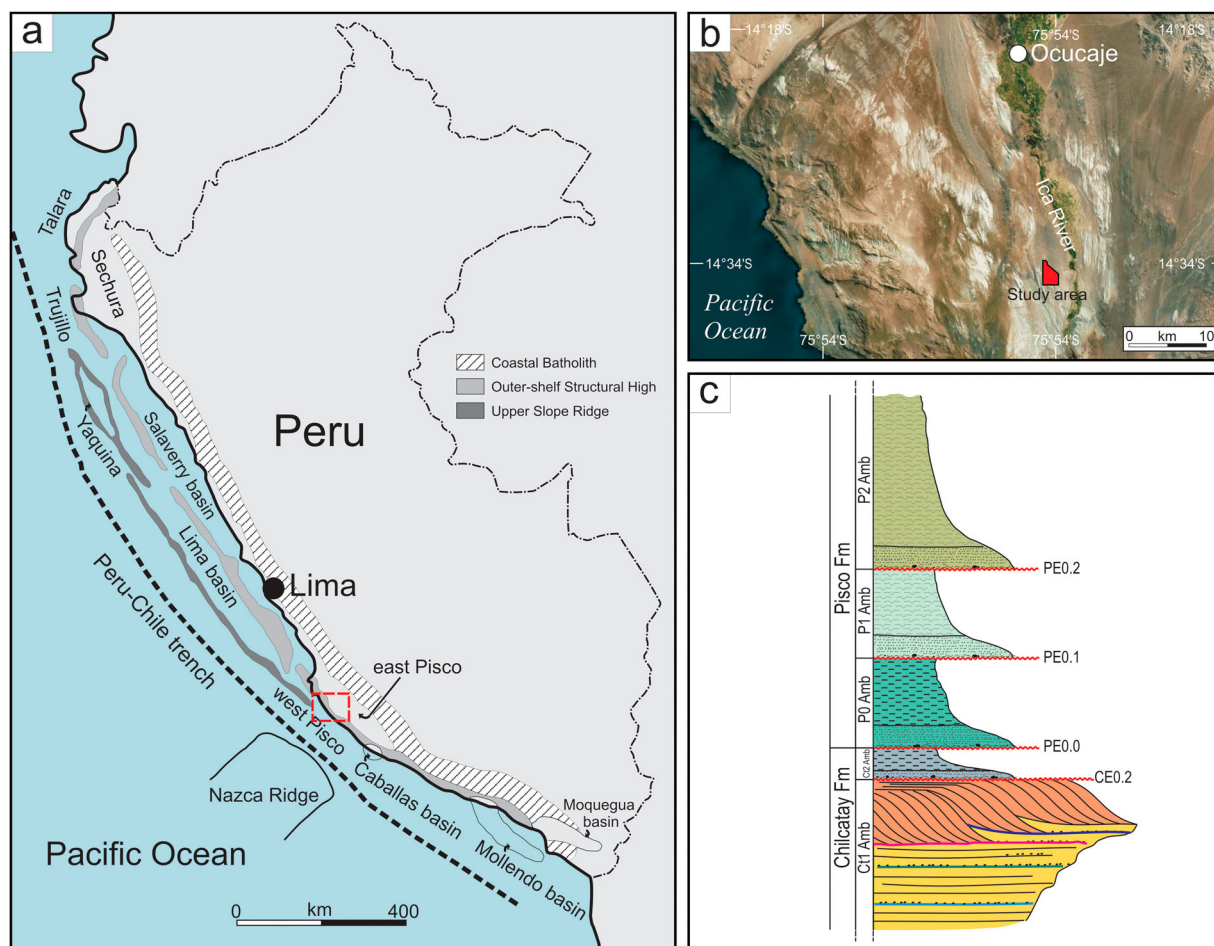
Figure 1. (a) Map of the major structural trends and basins of coastal Peru, redrawn and modified from Travis, Gonzales, and Pardo (1976) and Thornburg and Kulm (1981). The red dashed rectangle outlines location of the area shown in detail in Figure 1(b); (b) close up of the red dashed inset box in Figure 1(a) showing the geographic location of the study area along the western side of the Ica River valley; (c) Schematic stratigraphic column with the main subdivisions and units (not to scale).

be separated into an inner set of shelf basins and a seaward set of slope basins. The (east) Pisco Basin is one of these shelf basins and extends along the southern Peru from Pisco to Nazca towns. During the Miocene, the basin was a shallow-water, semi-enclosed embayment protected to the west by a chain of islands (Marocco & de Muizon, 1988; the Gran Tablazo Archipelago of DeVries & Jud, 2018) possibly of the emerging Outer-shelf Structural High. The basin fill consists mainly of Eocene to Pliocene sediments that, from oldest to youngest, have been subdivided into the Caballas Formation, the Paracas Formation (including the Los Choros and Yumaque members), the Otuma Formation, the Chilcatay Formation, and the Pisco Formation separated by basin-wide unconformities (DeVries, 1998; DeVries, 2017; DeVries & Jud, 2018; DeVries, Urbina, & Jud, 2017; Dunbar, Marty, & Baker, 1990).

3. Study area and methods

The study area is located some 55 km southwest of the Ica town and covers an area of approximately 5 km^2 near Ullujaya (Figure 1(b)). Physical stratigraphy and

architecture of the Chilcatay strata were documented through conventional geological field methods, including high-resolution sedimentological logging of a 66 m-long section, facies analysis, and geological mapping at 1:4000 scale (Main map). The stratigraphic analysis has been mainly carried out through the combined use of allostratigraphic (NACSN, 2005) and lithostratigraphic criteria, with unconformity-bounded allomembers as the fundamental units and lithostratigraphic units included to complement the allostratigraphic framework. A number of local key beds (Kb) and stratigraphic surfaces (Ks) were walked out across the study area. They were informally named KbD, KbC, KbB, KsA, in ascending stratigraphic order, and have proven particularly useful in correlating small outcrop areas with larger outcrops nearby and to place the vertebrate faunas in their correct relative stratigraphic positions.

As for Cerro Los Quesos and Cerro Colorado (Bianucci et al., 2016a, 2016b), two fossil-bearing localities of the upper Miocene Pisco Formation exposed in the same area, most of the vertebrate fauna was studied directly in the field and only a few highly significant specimens were collected and deposited at storage

facilities of the Museo de Historia Natural de la Universidad Nacional Mayor de San Marcos in Lima (MUSM). For each vertebrate specimen encountered during the survey, the geographic position was recorded by global positioning system and the stratigraphic position along the measured section was established in relation to at least two of the above mentioned key beds and stratigraphic surfaces with an accuracy ranging from ±0.4 to ±3 m.

Twenty-three sediment samples were collected along the measured section for biostratigraphic purposes. The samples were prepared as standard smear slides and analysed at 1000× with an Olympus BX50 polarised optical microscope. Radiometric dating was made on biotite crystals from a volcanic ash layer at the top of the Chilcatay Formation. Biotite crystals were analysed at the University of Milano-Bicocca and $^{40}Ar/^{39}Ar$ analyses were performed on handpicked biotite crystals using an updated procedure based on Villa, Hermann, Müntener, and Trommsdorff (2000).

4. The Chilcatay Formation

The Chilcatay Formation comprises marine diatomaceous and tuffaceous sandy siltstones, bioclastic sandstones and, along the base, massive sandstones, and large boulders of crystalline basement rocks. Based on planktonic foraminifera (Ibaraki, 1993) and diatoms found in Chilcatay strata exposed at Cerros Las Salinas and Cerro La Virgen, two localities about 100 and 70 km northwest of Ullujaya, a late Oligocene age has been assigned to the lowermost strata of this unit by DeVries and Jud (2018). Within the study area, the Chilcatay Formation is part of a gently dipping, northeast-facing monocline and its lower portion and base are not exposed. The Chilcatay Formation, however, a few kilometres south of Ullujaya rests on a pronounced angular unconformity on the Otuma Formation (DeVries & Jud, 2018) and disappears, possibly by onlap onto the basement rocks, a few kilometres to the north, defining a transgressive surface that becomes younger in the landward direction to the northeast. Internally, this unit has been resolved into two smaller sediment packages (allomembers) separated by a major intraformational unconformity (CE0.2) and informally designated Ct1 and Ct2 in stratigraphic order (Figures 1(c) and 2(a)).

4.1. Ct1 allomember

The measured portion of the Ct1 allomember is about 56 m thick and comprises two distinct lithosomes: (i) a sub-horizontal package of interbedded siltstones, sandy siltstones and medium- to fine-grained sandstones (*Ct1a* facies association); and (ii) a clinobedded package of coarse-grained deposits having a mixed siliciclastic-carbonate composition (*Ct1b* facies association).

4.1.1. Ct1 facies associations
Description. The bulk of the *Ct1a* facies association is characterised by the dominance of massive siltstones and medium- to fine-grained siliciclastic sandstones (Figure 2(b)). The diluted biogenic fraction is composed of small amounts of redeposited skeletal elements including barnacles and rarer calcareous tubes. Vertebrate material is abundant and includes disarticulated to partially articulated skeletons and isolated bones and shark teeth.

These fine-grained sediments are punctuated by discrete and laterally persistent beds of coarse-grained sandstones that range from 0.1 to 0.5 m in thickness and, locally, pass laterally into erosionally based granule- to boulder-sized conglomerates up to 1.5 m thick. The bases of these coarse-grained beds are sharp and display dense burrow assemblages comprising large *Thalassinoides* and subordinate *Gyrolithes* penetrating deeply into the subjacent fine-grained sediments (Figure 2(c, d)). The composition of the granule layers is a laterally variable mixture of siliciclastic grains and skeletal elements. The latter are mainly represented by broken or whole shells of barnacles, in particular cases similar to the genus *Austromegabalanus*, and mollusc shells (mainly pectinids but also ostreids). Rare encrusting bryozoans were observed on barnacle shells. Echinoid fragments and calcareous tubes are less common; rare benthic foraminifera are also present (Figure 3(a, b)). Cobble- to boulder-sized conglomerates are dominated by rounded clasts from an ash-flow tuff and the igneous basement set in a coarse-grained bioclastic matrix (Figure 3(c)).

Sediments of the *Ct1a* facies association underlie and, locally, landward interfinger (from southwest to northeast) with a 20 m-thick lithosome of mixed siliciclastic-carbonate deposits (*Ct1b* facies association) showing a conspicuous SW-directed progradational pattern. Field mapping demonstrates that the *Ct1b* prograding wedge is internally composite, consisting of a multilateral stack of clinobed packages. Clinoform height attains 15–20 m and maximum declivity ranges between 15° and 20°. Individual clinobeds are between 0.2 and 0.5 m thick and are composed of coarse-grained, well-sorted, skeletal-rich grainstones mixed with various amounts of granule- and small pebble-sized terrigenous components (compositional mixing *sensu* Chiarella, Longhitano, & Tropeano, 2017) (Figure 3(d)). The carbonate grain association is heterozoan (*sensu* James, 1997) and skeletal components include abundant barnacles and molluscs (Figure 3(e, f)); subordinate components are echinoids, calcareous tubes, and small benthic foraminifera. All shells show
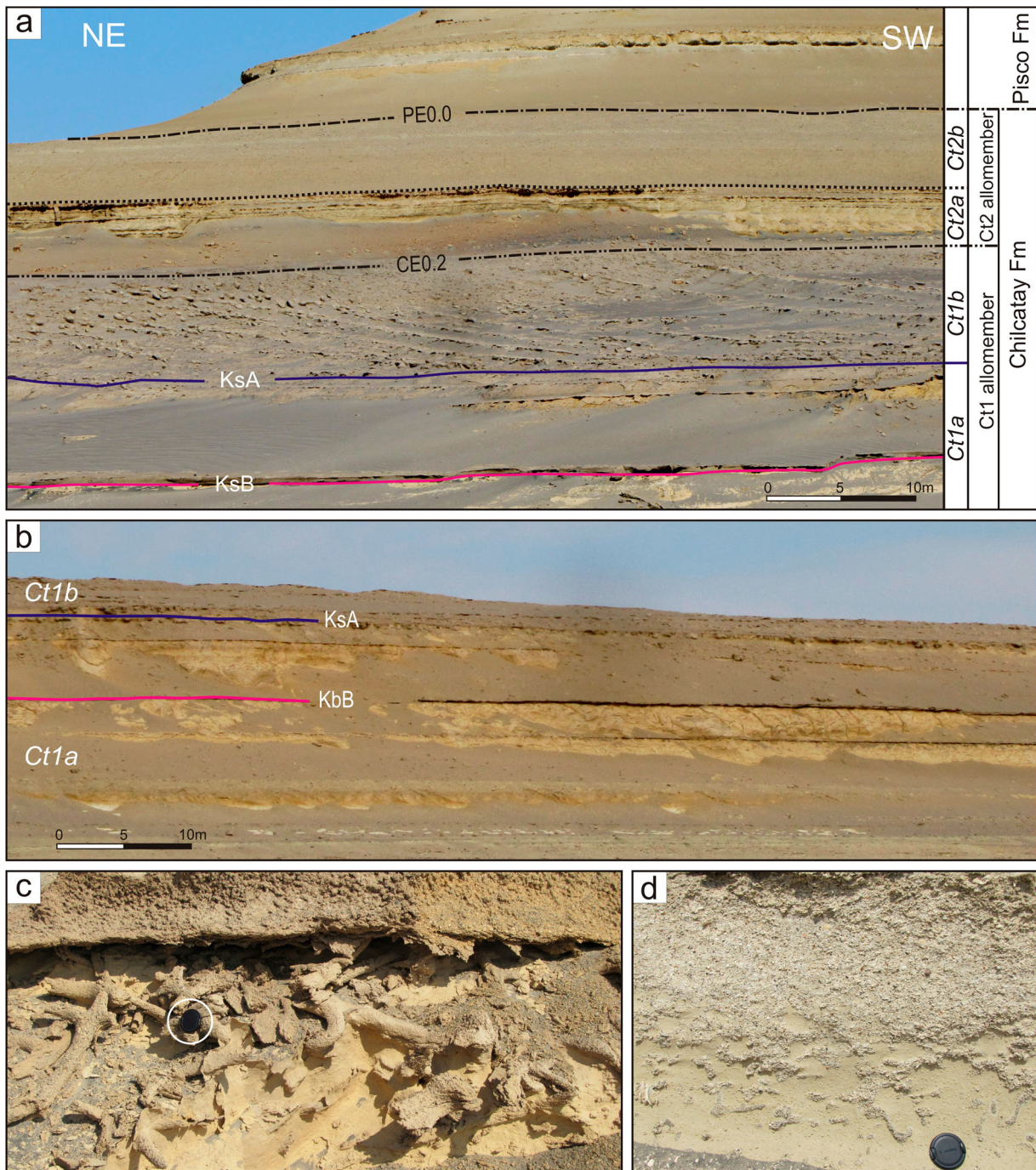
Figure 2. Representative outcrop views of the stratal architecture and some of the identified facies associations. (a) Depositional-dip oriented annotated panoramic photograph of the upper part of the Chilcatay Formation and the overlying Pisco Formation near Cerro Las Tres Piramides (14°35′22″S–75°38′20″W). The principal surfaces used to further subdivide the Chilcatay Formation into allomembers and the internal facies architecture are indicated. At this site, the *Ct1a* and *Ct1b* facies associations of the Ct1 allomember are separated by the KsA surface. Clinoforms of the *Ct1b* facies association prograde basinward, showing truncated tops and typical downlapping basal contact onto sub-horizontal finer-grained sediments of the *Ct1a* facies association. The Ct2 allomember rests on the CE0.2 unconformity and exhibits a strong retrogradational (fining-upward) facies trend. The Chilcatay and Pisco strata are separated by the PE0.0 unconformity; (b) panoramic view showing the contact (KsA) between sediments of the *Ct1a* facies association and the lowermost portion of the *Ct1b* facies association at Ullujaya (14°35′03″S–75°38′36″W). KbB is a granule-size conglomerate underlain by a conspicuous assemblage of *Thalassinoides* and *Gyrolithes* burrows; (c–d) Close-up views of a granule-size *Thalassinoides-Gyrolithes*-burrowed conglomerate beds. Note that subjacent silty strata are cut by a dense network of burrows that emanate from their bases and are passively filled with coarser-grained sediments from the immediately overlying event deposits.

a high degree of fragmentation and disarticulation and variably abraded shapes, indicative of transport. The lower boundary of the *Ct1b* clinoformed deposit is a downlap surface characterised by a sharp and undulated lithologic contact with underlying sediments of the *Ct1a* facies association (Figure 3(g, h)).
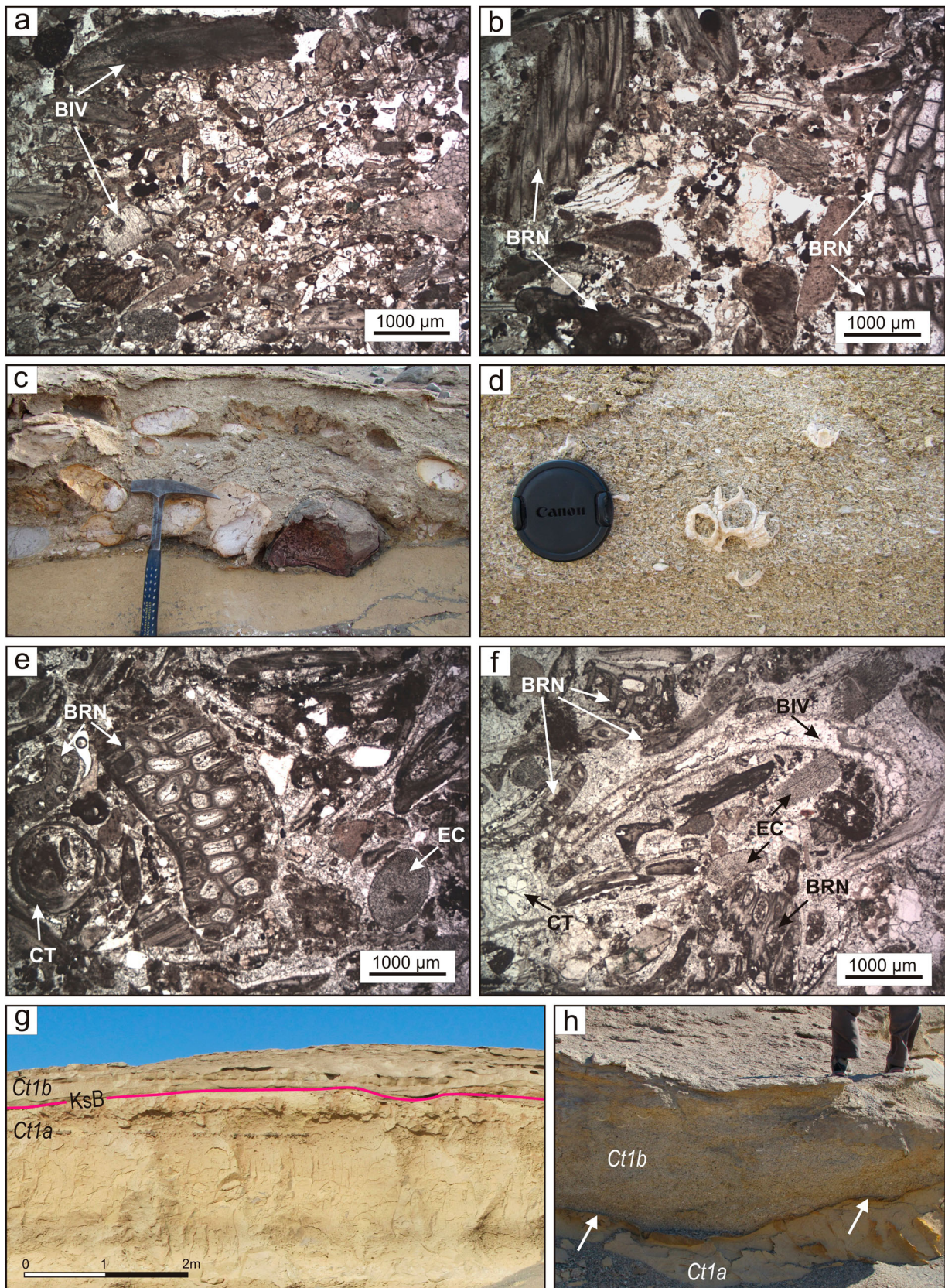
Figure 3. (a–b) Thin-section photomicrographs of a coarse-grained bed within *Ct1a* showing barnacles (BRN) and bivalves (BIV); (c) the conglomerates in *Ct1a* include rounded to sub-rounded, pebble- to cobble-sized clasts derived from the pre-Cenozoic basement units admixed with distinctive white-weathering, well-rounded clasts of an ash-flow tuff. Clasts are chaotically oriented and have a clast-supported texture with a skeletal-rich carbonate matrix indicating deposition by a gravity flow. A 30-cm-long rock hammer for scale; (d) a striking feature of the *Ct1b* mixed siliciclastic-carbonate deposits is their extreme coarseness, and the highly fragmental nature of their constituent particles. Macroscopically, they comprise a mixture of densely packed, gravel- and sand-sized skeletal detritus and terrigenous grains. Lens cap 6.5 cm in diameter; (e–f) thin-section photomicrographs of grain-supported fabrics in the lower portion of the *Ct1b* clinoforms composed of significant amounts of disaggregated barnacle plates (BRN) and bivalves (BIV), with echinoids (EC), calcareous tubes (CT) and benthic foraminifera being of secondary importance; (g) panoramic and (h) close up views of the undulated erosional contact marked by a sharp break in grain size between coarse-grained grainstones (transition-slope deposits, *Ct1b*) above and finer-grained sandy siltstones (offshore deposits, *Ct1a*) below.

Interpretation. The general stratigraphic architecture and skeletal composition of the *Ct1b* clinobedded lithosome described here reflect the outwards dispersal of carbonate sediment and bear striking similarities with seaward-prograding heterozoan carbonate wedges documented by Pomar and Tropeano (2001) and Massari and D'Alessandro (2012). According to these interpretations, they are thought to represent entirely submerged calcarenitic wedges (infralittoral prograding carbonate wedge, IPCW) having a storm-wave-graded profile and representing the progradation of distally steepened ramps dominated by physical accommodation in the sense of Pomar and Kendall (2008) (Figure 4). In this context, it is inferred that clinoform progradation resulted from intermittent transport of intensely reworked and winnowed coarse-grained skeletal hash and lithogenic particles from a shallow-marine carbonate factory, which was dominated by heterozoan skeletal components, onto a depositional frontal slope below the base level of storm waves (transition-slope setting of Pomar & Tropeano, 2001). Proximal to distal transport and dispersion of skeletal debris were especially active during storms by downwelling currents transforming into gravity flows at the clinoformed slope margin (Massari & Chiocci, 2006). At the same time, the finer sized particles were selectively swept away (winnowed) from the high-energy top of the prograding ramp and bypassed the clinoform slope as part of the suspended load to be deposited farther downdip, into a deeper inner shelf environment. The contemporary shallow-marine carbonate factory must have been situated towards the northeast, but is no longer preserved or exposed, leaving the prograding skeletal carbonate sediments as the only evidence for its existence.

Basinward, these clinoformed grainstones downlap onto and interfinger with the vertebrate fossil-bearing sediments of the *Ct1a* facies association. Given their downdip position with respect to the progradational carbonate wedge, the *Ct1a* facies association is considered to represent deposition by suspension fallout of shoreface-derived fine-grained material in an offshore depositional setting. The sharp-based sandstone and granule- to cobble-sized conglomerate beds interbedded into these fine-grained background sediments clearly reflect periodic high-energy events in otherwise quiet marine offshore settings. Accordingly, they are interpreted as event beds resulting from storm-induced, offshore-directed density currents transporting coarse-grained shoreface sediments beyond the toe of the transition slope.

4.2. Ct2 allomember

The calcarenitic wedge of the Ct1 allomember is unconformably overlain by a 10.5 m-thick, fining-upward unit that is virtually devoid of vertebrate fossils and is composed of basal sandstones (*Ct2a* facies association) gradually overlain by massive siltstones (*Ct2b* facies association).

4.2.1. Ct2 facies associations

Description. The basal surface of the Ct2 allomember (CE0.2) is typically penetrated by small *Thalassinoides* burrows crossing the topmost portion of the underlying clinobedded wedge. The overlying *Ct2a* facies association is about 3.5 m thick and consists of medium- to fine-grained, massive or weakly bedded, thoroughly bioturbated sandstones (Figure 2(a)). A thin pavement of small oysters and rare basement-derived pebble- and boulder-size clasts occurs at the base. Sediments are dominated by siliciclastic materials.

The *Ct2a* facies association grades upward into massive siltstones interbedded with dolomitised mudstone horizons and discrete volcanic ash layers, forming the *Ct2b* facies association. The siltstones are predominantly rich in carbonate microfossils (calcareous nannofossils and planktonic foraminifera) but become rich in siliceous microfossils (diatoms and silicoflagellates) in the upper portion.

Interpretation. The upward-fining pattern of the Ct2 allomember suggests an overall retrogradational (deepening-upwards) depositional trend with the basal *Ct2a* sandstones representing shoreface paleoenvironments and the finer-grained, tuffaceous, calcareous and diatomaceous *Ct2b* siltstones representing offshore paleoenvironments. The basement-derived pebble- and boulder-size clasts were probably introduced into the basin during periods of lowered sea level and imply a period of subaerial emergence prior to transgressive reworking. Accordingly, the basal CE0.2 bounding surface marks the turnaround from regression at the top of Ct1 to transgression at the base of Ct2 and is considered to represent a transgressively modified subaerial unconformity. The bioturbated nature of CE0.2 and its association with a basal oyster-bearing shelly horizon and lag gravel indicate that erosional scouring and shell concentration took place during a period of low or arrested deposition (e.g. Carnevale, Landini, Ragaini, Di Celma, & Cantalamessa, 2011; Kidwell, 1991; Kondo et al., 1998).

4.3. Chronostratigraphic framework

4.3.1. Microfossil biostratigraphy

Planktonic microfossils were studied from the samples collected along the measured section and in the area of Cerro Yasera de Amara, just outside of the study area (Table S1, providing species occurrence and ages of bioevents, is included in the supplementary material). It is important to highlight that: (i) ages of the considered diatom bioevents are based on Equatorial Pacific diatom biostratigraphy and may therefore not be
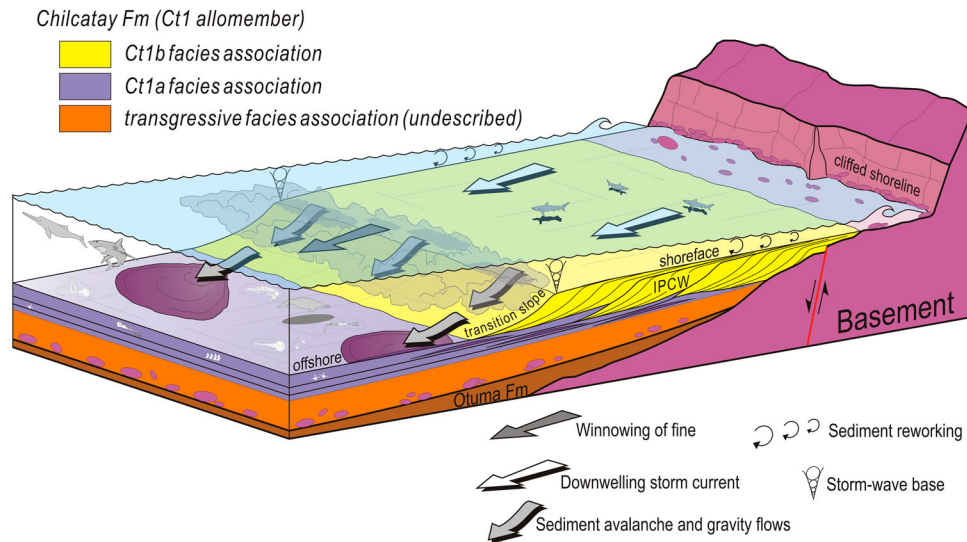
Figure 4. Block diagram (not to scale) illustrating interpreted depositional setting and relative positions of facies associations identified in the present study for the Ct1 allomember of the Chilcatay Formation at Ullujaya (modified from Pomar & Tropeano, 2001). Along the basin margin, extensive outcrops of basement rocks and residual gravels were sites of active skeletal production, providing the rugged, rocky substrates, and coarsely particulate bottoms preferred by most sedentary benthic organisms, such as barnacles and epifaunal bivalves (mostly ostreids and pectinids). Excess skeletal material produced by the shallow-water carbonate factory was intensely reworked and winnowed out by storm-induced waves and downwelling currents and dislodged basinwards to be either deposited along the clinoform slope (transition slope) on the front of the infralittoral prograding carbonate wedge (IPCW) by avalanches processes or dispersed over the surrounding offshore settings by suspension fallout and density flows.

fully representative of first and last occurrences at the Pisco Basin latitudes; (ii) ages of the considered silicoflagellate biozones have not been calibrated but correlated with nannofossil biozones.

Ct1a *facies association:* Diatoms include rare occurrences of *Rhaphidodiscus marylandicus* and *Triceratium pileus*, the latter constrained between 18.27 and 17.35 Ma (Expedition 320/321 Scientists, 2010) or between 18.06 and 17.89 (Barron, 2005). Rare occurrences of a form of *Coscinodiscus rhombicus*, possibly a transitional form to *C. lewisianus*, point to an age close to its last occurrence, dated at 18.44 Ma (Expedition 320/321 Scientists, 2010). Following diatom stratigraphy, samples from the *Ct1a* facies association are therefore assigned to the *Craspedodiscus elegans* zone (Expedition 320/321 Scientists, 2010). Silicoflagellates only occur in six samples collected at 24–27 m from the base of the section. Overall, they are rare but represented by a varied assemblage, assigning the samples to the upper part of the *Naviculopsis ponticula* zone (Bukry, 1981, 1985; Perch-Nielsen, 1985), which was dated at 18–19 Ma by correlation with calcareous nannofossil NN3 biozone (Bukry, 1982). Among nannofossils, rare occurrences of *Discoaster druggi* support this age assignment. These ages are consistent with those provided by DeVries (1998).

At Roca Negra, a locality about 7 km south of Ullujaya, recent investigations (Lambert et al., 2017) have documented the occurrence of a biostratigraphically informative silicoflagellate assemblage from the basal portion of the Chilcatay Formation. This assemblage, assigned to the *Naviculopsis ponticula* zone of Bukry (1981), contains species that are typical of the lower part of this biozone, thus implying a slightly older age then the strata outcropping in our study area. This new early Miocene age assignment for the base of the Chilcatay Fm is not in conflict with the late Oligocene age provided by DeVries and Jud (2018). From a basin-wide perspective, indeed, this chronostratigraphic reconstruction implies a time-transgressive nature of the formation boundary throughout the region, ranging from late Oligocene to early Miocene, when the maximum flooding of the shelf basin was reached. Accordingly, due to the diachronous character of the basal boundary and the marginal position of the study area along the eastern, internal flank of the basin, the base of the Chilcatay strata exposed at Ullujaya can be significantly younger than in other parts of the basin.

Ct1b *and* Ct2a *facies associations*: These two units are barren.

Ct2b *facies association*: Apart from abundant long-ranging species, the calcareous nannofossil assemblage is characterised by rare occurrences of *Sphenolithus belemnos*, constraining the age of the samples to 19.01–17.96 Ma. In the upper 4 m of *Ct2b*, as measured east of Cerro Yasera de Amara, silicoflagellates show a well-preserved assemblage and the notable absence of *Naviculopsis*, indicating that the samples are located above the LO of this genus, occurring at ca. 18 Ma, and therefore are assigned to the *Corbisema triacantha* zone. Rare specimens of *Coscinodiscus lewisianus* var. *similis* occur in the uppermost sample, which would restrict the age of the sample to younger than

17.8 Ma (*C. rhombicus* here is rather a transition form to *C. lewisianus* var. *similis*). We interpret the Ct2b diatom association as belonging to the *T. pileus* zone (17.49–18.18 Ma).

4.3.2. Isotope geochronology

An ash layer (SOT-T3) was collected in the upper part of *Ct2b* facies association, just 1 m below the erosional contact with the overlying Pisco Formation (14° 35'40.83"S–75°40'4.70"W). Electron probe micro-analyser analyses on biotite crystals exhibit a homogeneous population and do not show any K loss in the interlayer occupancy. The most reliable estimate of the biotite age is provided by the steps with the lowest Ca/K ratios, as the stoichiometry of biotite is Ca-free. A strict adherence to the definition of 'isochemical steps' (Villa, Ruggieri, Puxeddu, & Bertini, 2006) requires only considering steps 3–5, with Ca/K < 0.035. These steps give a mean weighted age of 17.99 ± 0.10 Ma and an isochron with atmospheric intercept. This age is nearly identical to that obtained by Belia and Nick (2016) with the $^{40}Ar/^{39}Ar$ method on the same ash (i.e. 17.70 ± 0.24 Ma). However, if one considers also steps 6–8, which have slightly higher Ca/K and Cl/K ratios (in any case Ca/K < 0.093), the resulting weighted average age is 18.02 ± 0.07 Ma, indistinguishable from the strict isochemical age, with a statistically acceptable dispersion (MSWD = 0.90), and also corresponding to an isochron with atmospheric intercept. The 18.02 ± 0.07 Ma estimate for SOT-T3 includes a higher number of steps and is slightly more precise than the 17.99 ± 0.10 Ma age estimate reported by Di Celma et al. (2017) for the same layer. The age spectrum displaying both options, the isochron and the Ca diagram are available in the supplementary materials.

5. Marine vertebrates

Eighty-two marine vertebrate specimens preserved as bony elements were recorded at Ullujaya.

Most of these fossils were found in a restricted area of about 1 km^2 and all fossils are from 9.7 to 33.5 m above the base of the examined section, representing a consistent portion of the 35-m-thick *Ct1a* facies association (Main map). Seventy-four specimens (97% of those with a stratigraphical collocation) are restricted in a 16.9-m-thick interval of sediments (13.9–30.8 m above the base). The largest concentrations along the section are around 14–15 m (22 specimens, 29%) and from 25 to 31 m (39 specimens, 51%). Fossil vertebrates were not found either in the Ct1b facies association or in the Ct2 allomember of the Chilcatay Fm exposed, both within the study area and in other prospected surrounding areas.

These marine vertebrate specimens consist of more or less disarticulated skeletons, all lacking at least some bones (Figure 5). Cetacean remains dominate the assemblage (86.6% of the specimens), with all specimens identifiable to suborder level belonging to Odontoceti (toothed cetaceans).

Excluding the indeterminate remains (56.1%), odontocetes were referred to Kentriodontidae (19.6%), Squalodelphinidae (6.1%), Physeteroidea (2.4%), and to the archaic long-snouted homodont odontocete *Chilcacetus cavirhinus* (2.4%).

Kentriodontids were referred to a small odontocete having generic affinities with *Kentriodon pernix* from the early Miocene of the Calvert Formation (USA; Kellogg, 1932). Being likely the most common cetacean from the Chilcatay Fm (pers. observation), this small stem Delphinida is represented at Ullujaya by several skulls (six collected and under study: MUSM 586, 631, 1393, 1397, 1398), in a few cases associated to partial postcrania. All these remains are found from 14.2 to 30.8 m above the base, indicating that this small delphinoid was coeval with the other odontocetes identified at Ullujaya.

Squalodelphinids include: (1) the holotype (MUSM 1396) and the referred specimen (MUSM 1403) of *Huaridelphis raimondii*, both represented by a skull, with some postcranial bones in MUSM 1403 (Lambert et al., 2014); (2) a well-preserved skull and associated cervical vertebra (MUSM 1395) described and referred to *Notocetus vanbenedeni* by Bianucci et al. (2015); (3) two indeterminate specimens consisting of a disarticulated skeleton (Figure 5(a)) (only the left tympanic bulla, one tooth and one humerus collected: MUSM 1484), and an isolated tympanic bulla (MUSM 1485).

Physeteroids consist of two isolated skulls, of which the best-preserved was collected and prepared (MUSM 3246) and is now under study. It exhibits some affinities with *Diaphorocetus poucheti* from the early Miocene Monte León Formation (Argentina; Moreno, 1892). Still in the field and rather damaged by erosion, a second physeteroid skull has previously been erroneously identified as a mysticete (Bianucci et al., 2015; Lambert et al., 2014), a mistake corrected via partial preparation in the field during September 2016.

Finally, two skulls with associated partial postcrania belong to *Chilcacetus cavirhinus*: specimen MUSM 1401 (described together with the holotype by Lambert et al., 2015) and another collected specimen (MUSM 2527) now under study.

Bony fish are uniformly distributed from 14.2 to 29.2 m above the base of the section. They are represented by several fragmentary specimens, consisting of an indeterminate skull and some tuna-like skull bones and segments of vertebral columns (Figure 5 (b)) and a partial postcranial skeleton of a large istiophorid billfish (tentatively referred to as cf. *Makaira* sp.). A large dermochelyid marine turtle, represented by a single specimen consisting of postcranial bones, was found 14.8 m above the base of the section.
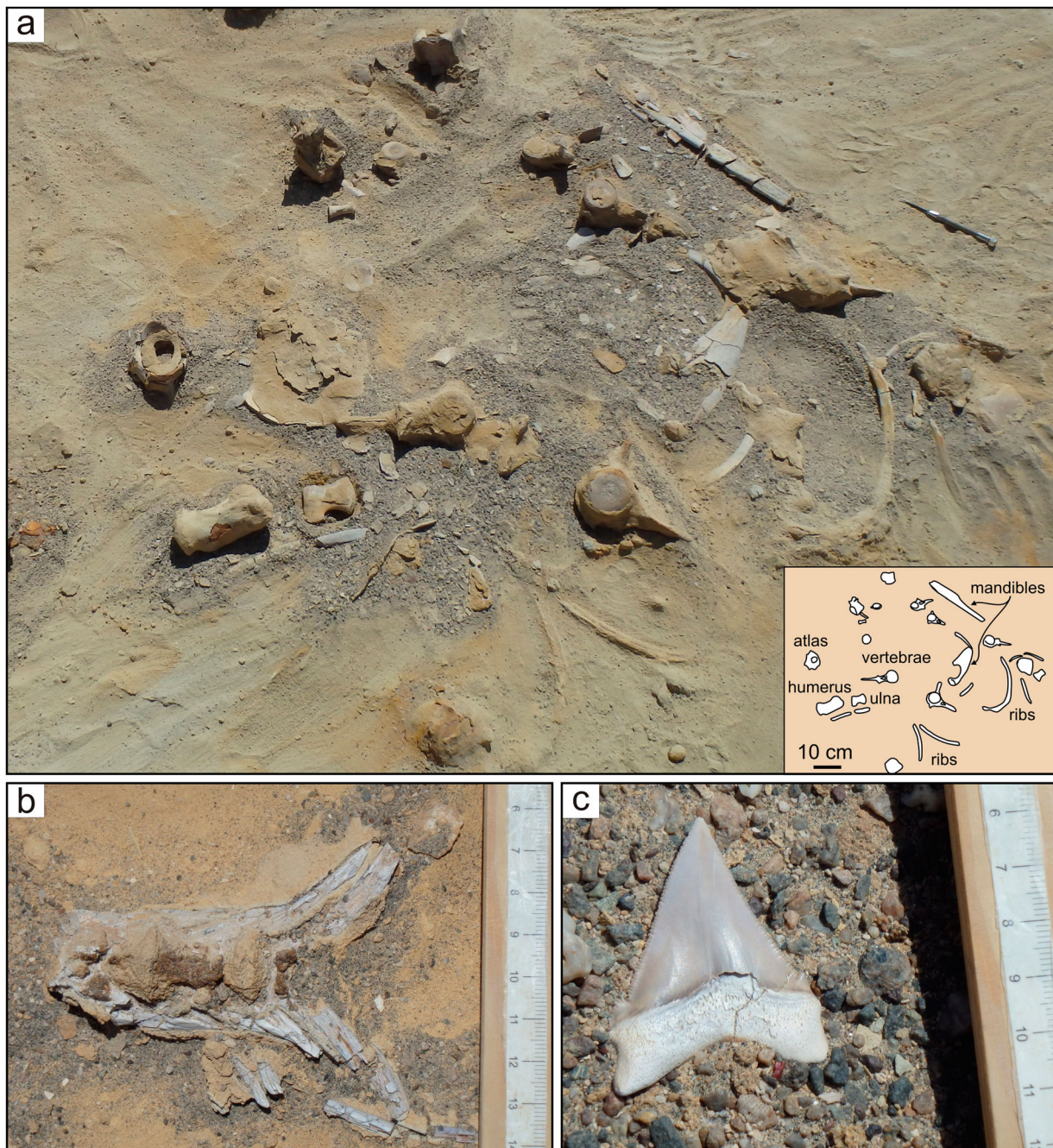
Figure 5. Fossil vertebrates from *Ct1a* facies association. (a) Disarticulated skeleton of Squalodelphinidae indet. (toothed whale); (b) caudal fin of cf. *Thunnus* sp. (bony fish); (c) tooth of *Carcharocles chubutensis* (shark).

More than one thousand isolated elasmobranch teeth and spines have been also collected at Ullujaya. They belong to the following orders: Carcharhiniformes (57.1% of the teeth), including carcharhinids (56.1%), hemigaleids (0.9%), and sphyrnids (0.1%); Lamniformes (35.2%), including lamnids (30.3%), otodontids (2.8%), alopiids (1.9%), and odontaspidids (0.2%); Myliobatiformes (7.5%); and Rhinopristiformes (0.2%) (Figure 5). Almost half of the elasmobranch specimens consist of teeth of *Carcharhinus brachyurus*; teeth of *Cosmopolitodus hastalis* and *Isurus oxyrinchus* are also abundant. Most of the elasmobranch remains come from a single bed located about 23 m above the base of the section, whereas a few other specimens (mostly belonging to lamniform taxa) come from different horizons of the *Ct1a* facies association.

6. Conclusions

This paper is the first detailed and integrated account of the sedimentology, physical stratigraphy, and chronostratigraphy of the Chilcatay Formation exposed at Ullujaya and provides data about its marine vertebrate assemblage. The combination of a high-resolution geological and stratigraphic study with the prospection and mapping of fossil vertebrates allowed the placement of all the fossils on a geological map and along

a temporally constrained measured section, providing an accurate spatial and temporal context to this fossil-bearing site and the individual fossil findings.

Based on detailed mapping and facies analysis, the studied interval has been resolved into two unconformity-bounded allomembers informally designated Ct1 and Ct2 in stratigraphic order. Ct1 comprises two facies associations representing the progradation of laterally adjacent depositional environments: (i) the *Ct1b* facies association recording a distally steepened mixed siliciclastic-bioclastic ramp; and (ii) the *Ct1a* facies association recording the coeval deeper parts of the basin (offshore setting) receiving bypass suspended fines from the shallower ramp. All fossil vertebrates, mainly consisting of odontocete bones and shark teeth, came from this facies association. Ct2 transgressively overlies the Ct1 allomember at surface CE0.2 and consists of two major facies associations comprising shoreface sandstones (*Ct2a*) and offshore silty facies (*Ct2b*).

Integration of biostratigraphic and ^{40}Ar/^{39}Ar age determinations provided robust age constraints to the two identified allomembers. Biostratigraphic data suggest deposition of the *Ct1a* sediments between 19 and 18 Ma, in particular closer to 18.4 Ma around 24–27 m from the base of the section. The *Ct2b* calcareous portion cannot be further constrained than the 19.01–17.95 Ma interval but the upper portion of the diatomaceous layer is dated around 18 Ma. The ^{40}Ar/^{39}Ar radiometric age of an ash layer from the uppermost portion of the Ct2 allomember indicates deposition at 18.02 ± 0.07 Ma; the differences with the biostratigraphic age can be probably explained as due to possible discrepancies in diatom calibration between the Equatorial Pacific and the Pisco Basin and poor calibration of silicoflagellate bioevents.

Reported here is a combined quantitative and qualitative evaluation of the distribution of the marine vertebrates from the Ct1 allomember. More generally, this study provides a first census of the richness and abundance of the marine vertebrate fossil assemblage of the Chilcatay Formation, and significant data about its vertical and spatial distribution. These results will be very useful for future research addressed to a better definition of the genesis of this important fossil vertebrate assemblage, advancing the knowledge of crucial steps of the evolutionary history of some marine vertebrate clades.

Software

The geological map was compiled by scanning hand drafts as black and white TIF files, and then digitising the linework using the Corel Draw X3 graphics package. By using the GIS Data processing application Global Mapper 12, contour lines for the 1:4000 scale topographic base map were generated from digital elevation models (DEMs) based on the Shuttle Radar Topography Mission 26 (SRTM) as released by the United States Geological Survey (SRTM3 USGS version 2.1).

Disclosure statement

No potential conflict of interest was reported by the authors.

References

Barron, J.A. (2005). Diatom biochronology of the early Miocene of the equatorial Pacific. *Stratigraphy*, 2, 281–309.

Belia, E. R., & Nick, K. E. (2016). Early-Miocene calcareous nannofossil biostratigraphy from low-latitude, Pisco Basin, Peru. *Geological Society of America Abstracts with Programs*, 48, 4.

Bianucci, G., Di Celma, C., Landini, W., Landini, W., Post, K., Tinelli, C., … Lambert, O. (2016a). Fossil marine

vertebrates of Cerro Los Quesos: Distribution of cetaceans, seals, crocodiles, seabirds, sharks, and bony fish in a late Miocene locality of the Pisco Basin, Peru. *Journal of Maps*, 12, 543–557. doi:10.1080/17445647.2015.1115785.

Bianucci, G., Di Celma, C., Collareta, A., Post, K., Tinelli, C., de Muizon, C., … Lambert, O. (2016b). Distribution of fossil marine vertebrates in Cerro Colorado, the type locality of the giant raptorial sperm whale *Livyatan melvillei* (Miocene, Pisco Formation, Peru). *Journal of Maps*, 12, 1037–1046. doi:10.1080/17445647.2015.1048315.

Bianucci, G., Urbina, M., & Lambert, O. (2015). A new record of *Notocetus vanbenedeni* (Squalodelphinidae, Odontoceti, Cetacea) from the early Miocene of Peru. *Comptes Rendus Palevol*, 14, 5–13. doi:10.1016/j.crpv.2014.08.003.

Brand, L., Urbina, M., Chadwick, A., DeVries, J. T., & Esperante, R. (2011). A high resolution stratigraphic framework for the remarkable fossil cetacean assemblage of the Miocene/Pliocene Pisco Formation, Peru. *Journal of South American Earth Sciences*, 31, 414–425. doi:10.1016/j.jsames.2011.02.015.

Bukry, D. (1981). Synthesis of Silicoflagellate stratigraphy for Maestrichtian to Quaternary marine sediments. In T. E. Warme, R. C. Douglas, & E. L. Winterer (Eds.), *The deep sea drilling project: A decade of progress* (pp. 433–444). Tulsa: SEPM, Special Publication, 32.

Bukry, D. (1982). *Cenozoic Silicoflagellates from offshore Guatemala, deep sea drilling project site 495*. Initial Reports, DSDP 67: 425–445. Washington: U.S. Govt. Printing Office.

Bukry, D. (1985). Correlation of late Cretaceous Arctic silicoflagellates from Alpha Ridge. In H. R. Jackson, P. J. Mudie, & S. M. Blasco (Eds.), *Initial geological report on CESAR - the Canadian expedition to study the alpha ridge, arctic ocean. Geological Survey of Canada,* Paper 84–22, 125–135. doi:10.4095/120315.

Carnevale, G., Landini, W., Ragaini, L., Di Celma, C., & Cantalamessa, G. (2011). Taphonomic and paleoecological analyses (mollusks and fishes) of the Sua member condensed shellbed, Upper Onzole Formation (early Pliocene, Ecuador). *PALAIOS*, 26, 160–172. doi:10.2110/palo.2010.p10-070r.

Chiarella, D., Longhitano, S. G., & Tropeano, M. (2017). Types of mixing and heterogeneities in siliciclastic-carbonate sediments. *Marine and Petroleum Geology*, 88, 617–627. doi:10.1016/j.marpetgeo.2017.09.010.

DeVries, T. J. (1998). Oligocene deposition and Cenozoic sequence boundaries in the Pisco Basin. *Journal of South American Earth Sciences*, 11, 217–231. doi:10.1016/S0895-9811(98)00014-5.

DeVries, T. J. (2017). Eocene stratigraphy and depositional history near Puerto Caballas (East Pisco Basin, Peru). *Bol. Sociology Geology Perú*, 112, 39–52.

DeVries, T. J., & Jud, N. A. (2018). Lithofacies patterns and paleogeography of the Miocene Chilcatay and lower Pisco depositional sequences (East Pisco Basin, Peru). *Bol. Sociology Geology Perú*, Volumen Jubilar 8, 124–167.

DeVries, T. J., & Schrader, H. (1997). Middle Miocene marine sediments in the Pisco Basin (Peru). *Bol. Sociology Geology Perú*, 87, 1–13.

DeVries, T. J., Urbina, M., & Jud, N. A. (2017). The Eocene-Oligocene Otuma depositional sequence (East Pisco Basin, Peru): Paleogeographic and paleoceanographic implications of new data. *Bol. Sociology Geology Perú*, 112, 14–38.

Di Celma, C., Malinverno, E., Bosio, G., Collareta, A., Gariboldi, K., Gioncada, A., … Bianucci, G. (2017). Sequence stratigraphy and paleontology of the upper Miocene Pisco Formation along the western side of the lower Ica valley (Ica Desert, Peru). *Rivista Italiana di Paleontologia e Stratigrafia (Research in Paleontology and Stratigraphy)*, 123, 255–274. doi:10.13130/2039-4942/8373.

Di Celma, C., Malinverno, E., Cantalamessa, G., Gioncada, A., Bosio, G., Villa, I. M., … Bianucci, G. (2016a). Stratigraphic framework of the late Miocene Pisco Formation at Cerro Los Quesos (Ica Desert, Peru). *Journal of Maps*, 12, 1020–1028. doi:10.1080/17445647.2015.1115783.

Di Celma, C., Malinverno, E., Gariboldi, K., Gioncada, A., Rustichelli, A., Pierantoni, P. P., … Bianucci, G. (2016b). Stratigraphic framework of the late Miocene to Pliocene Pisco Formation at Cerro Colorado (Ica Desert, Peru). *Journal of Maps*, 12, 515–529. doi:10.1080/17445647.2015.1047906.

Dunbar, R. B., Marty, R. C., & Baker, P. A. (1990). Cenozoic marine sedimentation in the Sechura and Pisco basins, Peru. *Palaeogeography, Palaeoclimatology, Palaeoecology*, 77, 235–261. doi:10.1016/0031-0182(90)90179-B.

Expedition 320/321 Scientists. (2010). *Methods*. In H. Pälike, M. Lyle, H. Nishi, I. Raffi, K. Gamage, A. Klaus, and the Expedition 320/321 Scientists, Proceedings of the integrated ocean drilling program, 320/321: Tokio: Integrated Ocean Drilling Program Management International, Inc.. doi:10.2204/iodp.proc.320321.102.2010.

Gariboldi, K., Bosio, G., Malinverno, E., Gioncada, A., Di Celma, C., Villa, I. M., … Bianucci, G. (2017). Biostratigraphy, geochronology and sedimentation rates of the Upper Miocene Pisco Formation at two important marine vertebrate fossil-bearing sites of southern Peru. *Newsletters on Stratigraphy*, 50, 417–444. doi:10.1127/nos/2017/0345

Ibaraki, M. (1993). Eocene to early Miocene planktonic foraminifera from the south of Paracas, central Peru. Shizuoka University, *Report of the Faculty of Sciences*, 27, 77–93.

James, N. P. (1997). The cool-water carbonate depositional realm. In N. P. James & J. A. D. Clarke (Eds.), *Cool-water carbonates* (pp. 1–20). Tulsa: SEPM, Special Publication, 56.

Kellogg, R. (1932). A Miocene long-beaked porpoise from California. *Smithsonian Miscellaneous Collections*, 87, 1–11.

Kidwell, S. M. (1991). Condensed deposits in siliciclastic sequences: Expected and observed features. In G. Einsele, W. Ricken & A. Seilacher (Eds.), *Cycles and events in stratigraphy* (pp. 682–695). Heidelberg: Springer-Verlag.

Kondo, Y., Abbott, S. T., Kitamura, A., Kamp, P. J. J., Naish, T. R., Kamataki, T., & Saul, G. S. (1998). The relationship between shellbed type and sequence architecture: Examples from Japan and New Zealand. *Sedimentary Geology*, 122, 109–127. doi:10.1016/S0037-0738(98)00101-8.

Lambert, O., Bianucci, G., & Urbina, M. (2014). *Huaridelphis raimondii*, a new early Miocene Squalodelphinidae (Cetacea, Odontoceti) from the Chilcatay Formation, Peru. *Journal of Vertebrate Paleontology*, 34, 987–1004. doi:10.1080/02724634.2014.858050.

Lambert, O., de Muizon, C., & Bianucci, G. (2015). A new archaic homodont toothed whale (Mammalia, Cetacea, Odontoceti) from the early Miocene of Peru. *Geodiversitas*, 37, 79–108. doi:10.5252/g2015n1a4.

Lambert, O., de Muizon, C., Malinverno, E., Di Celma, C., Urbina, M., & Bianucci, G. (2017). A new odontocete (toothed cetacean) from the early Miocene of Peru expands the morphological disparity of extinct heterodont dolphins. *Journal of Systematic Palaeontology*. doi:10.1080/14772019.2017.1359689.

León, W., Aleman, A., Torres, V., Rosell, W., & De La Cruz, O. (2008). Estratigrafía, Sedimentología y evolución tectónica de la cuenca Pisco Oriental. *Boletín INGEMMET*, 27(Serie D), 144. Lima, Peru.

Marocco, R., & de Muizon, C. (1988). Le Bassin Pisco, bassin cénozoïque d'avant arc de la côte du Pérou central: Analyse géodynamique de son remplissage. *Géodynamique*, 3, 3–19.

Massari, F., & Chiocci, F. (2006). Biocalcarenite and mixed cool-water prograding bodies of the Mediterranean Pliocene and Pleistocene: architecture, depositional setting and forcing factors. In H. M. Pedley & G. Carannante (Eds.), *Cool-water carbonates: Depositional systems and palaeoenvironmental controls* (pp. 95–120). London: Geological Society, Special Publications, 255. doi:10.1144/GSL.SP.2006.255.01.08.

Massari, F., & D'Alessandro, A. (2012). Facies partitioning and sequence stratigraphy of a mixed siliciclastic-carbonate ramp stack in the Gelasian of Sicily (S Italy): A potential model for icehouse, distally-steepened heterozoan ramps. *Rivista Italiana di Paleontologia e Stratigrafia*, 118, 503–534. doi:10.13130/2039-4942/6017.

Moreno, F. P. (1892). Noticias sobre algunos cetáceos fósiles y actuales de la República Argentina. *Revista del Museo de La Plata*, 3, 383–400.

North American Commission on Stratigraphic Nomenclature (NACSN). (2005). North American stratigraphic code. *American Association of Petroleum Geologists Bulletin*, 89, 1547–1591. doi:10.1306/07050504129.

Perch-Nielsen, K. (1985). Silicoflagellates. In H. M. Bolli, J. B. Saunders, & K. Perch-Nielsen (Eds.), *Plankton stratigraphy* (Vol. 2, pp. 811–846). Cambridge: Cambridge University Press.

Pomar, L., & Kendall, C. G. S. C. (2008). Architecture of carbonate platforms: A response to hydrodynamics and evolving ecology. In J. Lukasik & A. Simo (Eds.), *Controls on carbonate platform and reef development* (pp. 187–216). SEPM, Special Publication, 89. doi:10.2110/pec.08.89.0187.

Pomar, L., & Tropeano, M. (2001). The Calcarenite di Gravina Formation in Matera (southern Italy): New insights for coarse-grained, large scale, cross-bedded bodies encased in offshore deposits. *American Association of Petroleum Geologists Bulletin*, 85, 661–689.

Thornburg, T. M., & Kulm, L. D. (1981). Sedimentary basins of the Peru continental margin: Structure, stratigraphy, and Cenozoic tectonics from 6°S to 16°S latitude. In L. D. Kulm, J. Dymond, E. J. Dasch, & D. M. Hussong (Eds.), *Nazca plate: Crustal formation and Andean convergence* (vol. 154, pp. 393–422). Memoir: Geological Society of America.

Travis, R. B., Gonzales, G., & Pardo, A. (1976). Hydrocarbon potential of coastal basins of Peru. In M. Halbouty, J. Maher, and H. M. Lian (Eds.), *Circum-pacific energy and mineral resources* (Vol. 25, pp. 331–338). Tulsa: American Association of Petroleum Geologists Memoir.

Villa, I. M., Hermann, J., Müntener, O., & Trommsdorff, V. (2000). $^{39}Ar/^{40}Ar$ dating of multiply zoned amphibole generations (Malenco, Italian Alps). *Contributions to Mineralogy and Petrology*, 140, 363–381. doi:10.1007/s004100000197.

Villa, I. M., Ruggieri, G., Puxeddu, M., & Bertini, G. (2006). Geochronology and isotope transport systematics in a subsurface granite from the Larderello-Travale geothermal system (Italy). *Journal of Volcanology and Geothermal Research*, 152, 20–50. doi:10.1016/j.jvolgeores.2005.09.011.

Wright, R., Dunbar, R. B., Allen, M., & Baker, P. (1988). Morphology of stacked marine delta lobes, East Pisco Basin, Peru. In A. W. Bally (Ed.), *Atlas of seismic stratigraphy* (pp. 192–196). Tulsa: AAPG, Studies in Geology, #27, v. III.